



Willems, C. J.L., Vondrak, A., Munsterman, D. K., Donselaar, M. E. and Mijnlief, H. F. (2017) Regional geothermal aquifer architecture of the fluvial Lower Cretaceous Nieuwerkerk Formation – a palynological analysis. *Netherlands Journal of Geosciences*, 96(4), pp. 319-330.

There may be differences between this version and the published version. You are advised to consult the publisher's version if you wish to cite from it.

<http://eprints.gla.ac.uk/157217/>

Deposited on: 16 March 2018

Enlighten – Research publications by members of the University of Glasgow_
<http://eprints.gla.ac.uk>

1 Regional geothermal aquifer architecture of the fluvial Lower Cretaceous Nieuwerkerk 2 Formation - a palynological analysis

3
4 C.J.L.Willems - *Department of Geoscience and Engineering, Delft University of Technology, Delft, Netherlands, willems.cjl@gmail.com*
5 A. Vondrak - *PanTerra Geoconsultants B.V., Leiderdorp, the Netherlands, A.Vondrak@panterra.nl*
6 D.K. Munsterman - *TNO – Geological Survey of the Netherlands, Utrecht, the Netherlands, dirk.munsterman@tno.nl*
7 M.E. Donselaar - *Department of Geoscience and Engineering, Delft University of Technology, Delft, Netherlands, m.e.donselaar@tudelft.nl*
8 H.F. Mijnlief - *TNO – Geological Survey of the Netherlands, Utrecht, the Netherlands, Harmen.Mijnlief@tno.nl*

9
10 corresponding author: C.J.L. Willems: willems.cjl@gmail.com
11

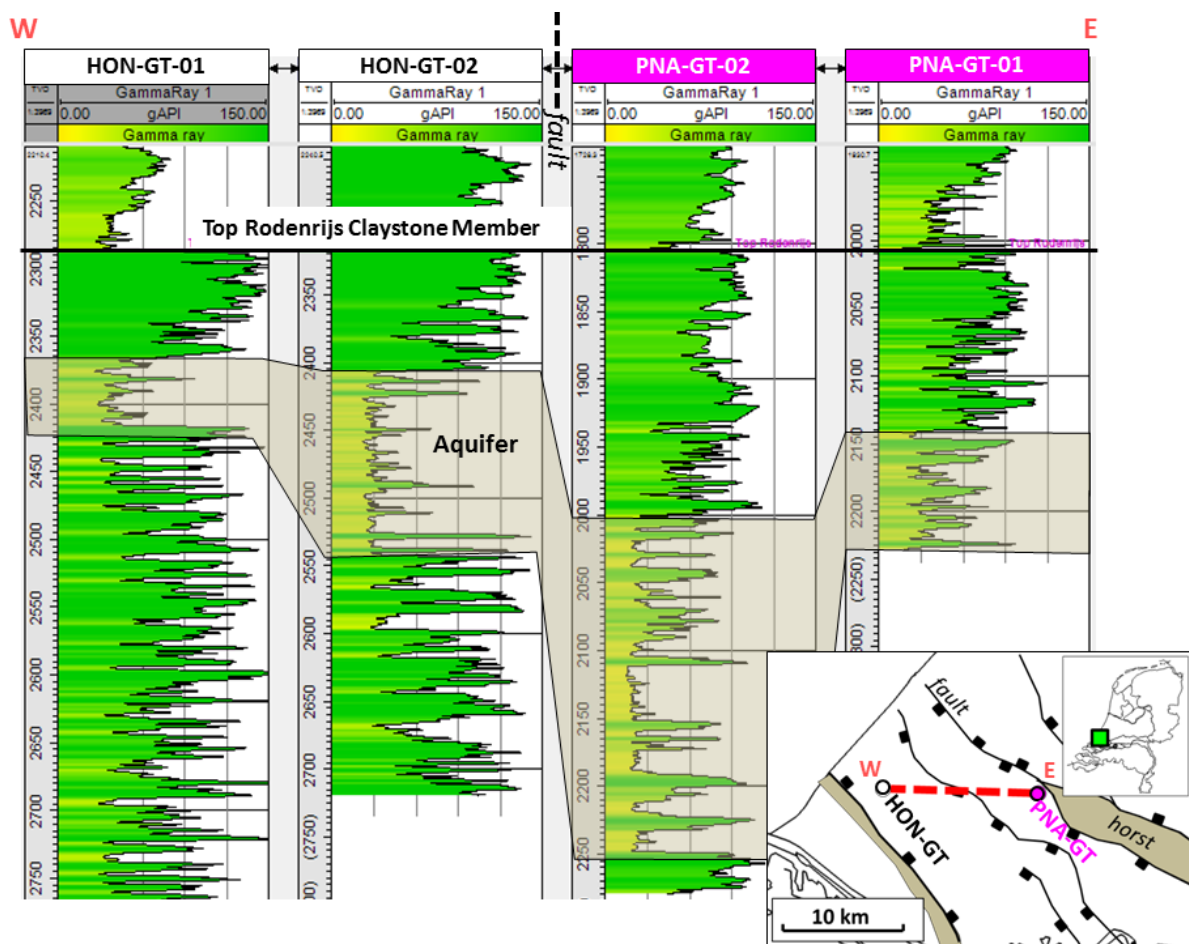
12 13 **Abstract**

14 The primary challenge for efficient geothermal doublet design and deployment is the adequate prediction of the
15 size, shape, lateral extent and thickness (or: aquifer architecture) of aquifers. In the West Netherlands Basin,
16 Lower Cretaceous sandstone-rich successions form the main aquifers for geothermal heat exploitation. Large
17 variations in the thickness of these successions are recognised in currently active doublet systems that cannot be
18 explained. This creates an uncertainty in aquifer thickness prediction, which increases the uncertainty in doublet
19 lifetime prediction as it has an impact on net aquifer volume. The goal of this study was to improve our
20 understanding of the thickness variations and regional aquifer architecture of the Nieuwerkerk Formation
21 geothermal aquifers. For this purpose new palynological data were evaluated to correlate aquifers in currently
22 active doublet systems based on their chronostratigraphic position and regional Maximum Flooding Surfaces.
23 Based on the palynological cuttings analysis, the fluvial interval was subdivided into two successions; a Late
24 Ryazanian to Early Valanginian succession and a Valanginian succession. Within these successions trends were
25 identified in sandstone content. In combination with seismic interpretation, maps were constructed that predict
26 aquifer thickness and their lateral extent in the basin. The study emphasises the value of palynological analyses
27 to reduce the uncertainty of fluvial Hot Sedimentary Aquifer exploitation.
28
29
30

31 **Keywords:** Direct-use geothermal, Hot Sedimentary Aquifers, Nieuwerkerk Formation, Sporomorph Eco-
32 Grouping, West Netherlands Basin.
33
34
35
36
37
38
39
40
41
42

43 **Introduction**

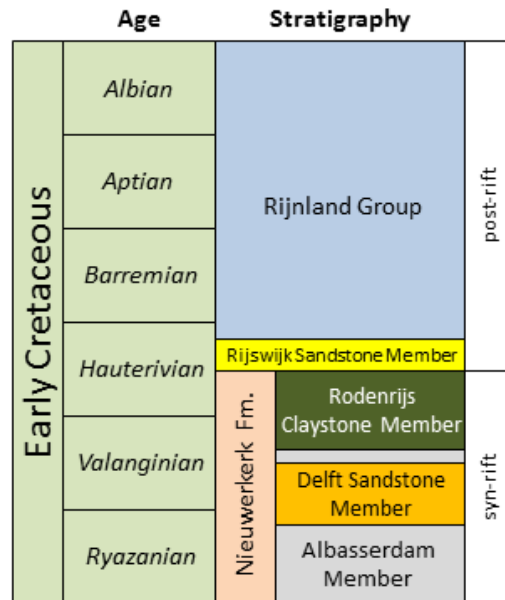
44 In geothermal exploitation of sedimentary rocks, it is crucial to adequately predict the regional aquifer
45 distribution. Often geological data is sparse and property extrapolation is required over large distances.
46 This is especially challenging for fluvial aquifers, which are notorious for lateral variation in lithofacies and
47 aquifer properties. The prediction of the regional sandstone distribution (henceforth fluvial architecture) from
48 well logs in fluvial aquifers is often ambiguous because lithofacies distribution could be affected by both
49 allogenic and autogenic processes (e.g., Hajek et al., 2010; Donselaar et al., 2013; Flood and Hampson, 2015;
50 Van Toorenburg et al., 2016). This is reflected by large aquifer thickness variations that are recognised in
51 currently active geothermal doublet wells in the West Netherlands Basin (WNB). The fluvial, sandstone-rich
52 successions that form the aquifer of the geothermal HON-GT doublet range in thickness from 50 to 150 m in
53 approximately 1.5 km spaced wells (Figure 1). In addition, the depth of this aquifer below the top of the
54 marginally marine Rodenrijs Claystone Member (e.g. Van Adrichem Boogaert and Kouwe, 1993) ranges from
55 almost 100 m to more than 200 m in different geothermal wells. Up to now, these variations cannot be explained
56 and create uncertainty in the prediction of lifetime and drilling costs of future doublet systems in the WNB.
57



58
59 *Figure 1: Gamma-ray logs of two geothermal doublets HON-GT and PNA-GT. Fault interpretation is based on Duin et al.*
60 *(2006). Well-log correlation is based on 'End-of-well reports' (NLOG, 2017).*

61
62

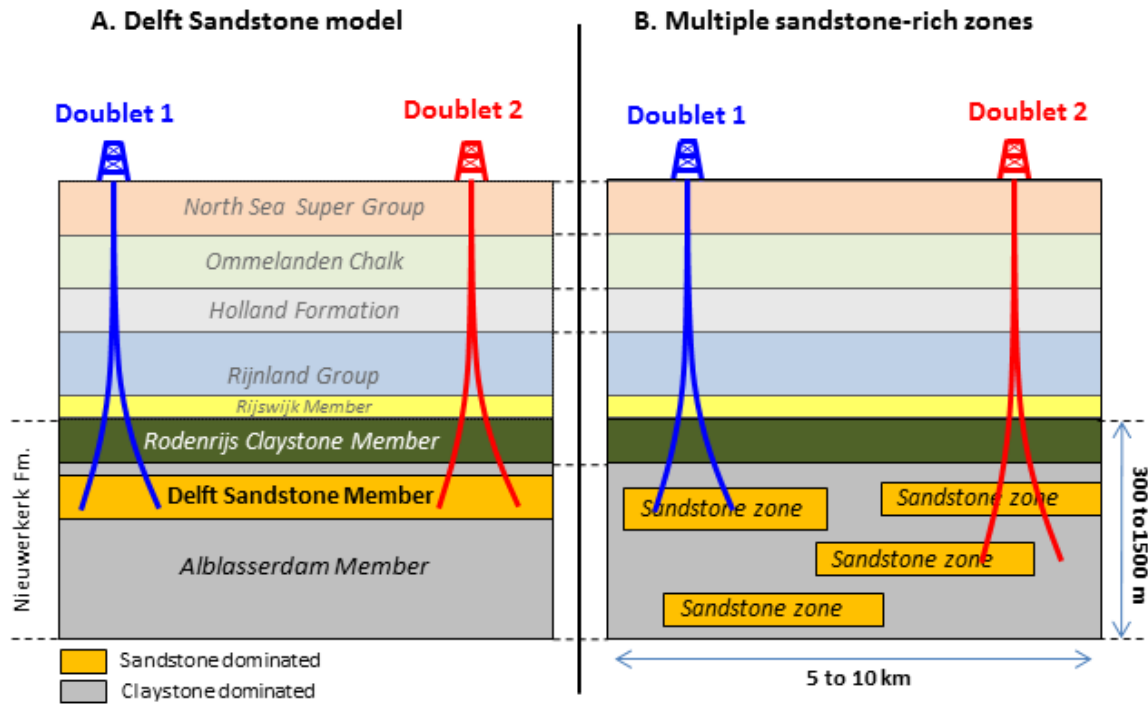
63 The aquifer in the geothermal wells of Figure 1 is interpreted as the Delft Sandstone Member which is
 64 part of the Lower Cretaceous Nieuwerkerk Formation (e.g., Van Adrichem Boogaert and Kouwe,
 65 1993; Den Hartog Jager, 1996; Herngreen and Wong, 2007, Donselaar et al., 2015). This member is
 66 characterised as a syn-rift, sandstone-rich interval ranging in age from Valanginian to Early
 67 Hauterivian, deposited in a meandering fluvial environment. Regional transgression and subsidence
 68 resulted in an increasingly marine character of the overlying sediments ranging from the restricted
 69 marine Rodenrijs Claystone Member to the marine Rijnland Group (Figure 2).
 70



71
 72 *Figure 2: Stratigraphic column for the Early Cretaceous section in the WNB indicating tectonic activity during deposition of*
 73 *the Rijnland Group, the Nieuwerkerk Formation and the main geothermal aquifers in the WNB: the Rijswijk Sandstone*
 74 *Member and the Delft Sandstone Member (Van Adrichem Boogaert and Kouwe, 1993).*
 75

76 The interpretation of the Delft Sandstone Member as a single sandstone-rich interval in the upper
 77 section of the Nieuwerkerk Formation (Figure 3-A) is derived from lithostratigraphic regional well-log
 78 correlation from numerous hydrocarbon wells in the WNB (e.g., Racero-Baena and Drake, 1996;
 79 Herngreen and Wong, 2007). This model is commonly used in geothermal exploitation in the basin for
 80 doublet design and deployment. However, recent regional stratigraphic studies based on sequence
 81 stratigraphic principles did not acknowledge the Delft Sandstone Member (DeVault and Jeremiah,
 82 2002; Jeremiah et al., 2010). DeVault and Jeremiah (2002) state that because of the syn-rift origin of
 83 the Nieuwerkerk Formation, clusters of amalgamated sandstone-rich zones can exist throughout the
 84 Nieuwerkerk Formation that not necessarily form one single, continuous sandstone-rich interval
 85 (Figure 3-B). The existence of two geological models that describe sandstone distribution in the
 86 Nieuwerkerk Formation creates uncertainty for geothermal exploitation because both models have a
 87 different impact on possible interference and aquifer thickness prediction. If the aquifer is formed by a
 88 single continuous sandstone-rich interval, pressure communication could affect injectivity and
 89 productivity of adjacent doublets, as is illustrated in Figure 3-A. In contrast, pressure communication
 90 is less straightforward if different sandstone-rich zones occur with limited lateral extent. In the
 91 example of Figure 3-B, claystone-dominated zones can form flow barriers or baffles between doublets
 92 1 and 2. Furthermore, when the aquifer is not formed by a single sandstone-rich zone, the aquifer
 93 thickness depends on the lateral extent of the sandstone-rich zones that the doublets can encounter as
 94 is illustrated for doublet 2 in Figure 3-B. Furthermore, the model in Figure 3-B suggests that multiple

95 aquifer targets can be present at deeper and hotter stratigraphic intervals affecting the geothermal
 96 potential in the region.
 97
 98
 99



100
 101 *Figure 3: (A) Cartoons illustrating the difference in sandstone distribution in the Nieuwerkerk Formation in schematic strike*
 102 *sections on graben scale according to (A) the Delft Sandstone model and (B) the multiple sandstone-rich zones models.*

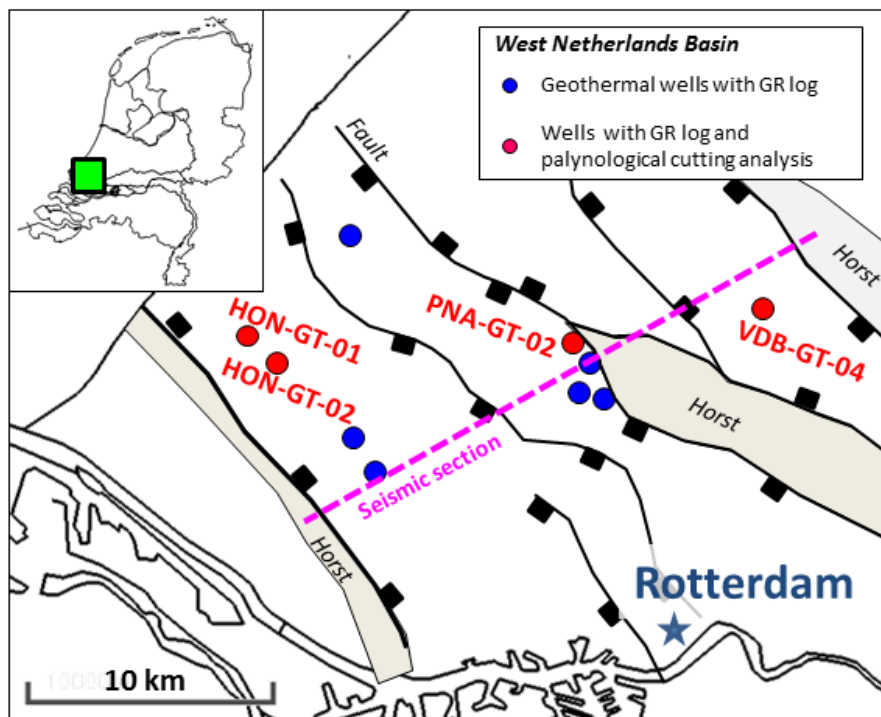
103
 104 The goal of this study is to place the fluvial aquifers in a chronostratigraphic framework. The results
 105 should decrease the uncertainty in the prediction of aquifer thickness for new doublet systems in the
 106 WNB and contribute to optimised doublet design. To reach this goal, palynological samples from drill
 107 cuttings are analysed in three geothermal wells: HON-GT-01, HON-GT-02, and PNA-GT-02 to define
 108 the chronostratigraphic position of fluvial intervals and identify regional Maximum Flooding Surfaces
 109 (MFS's). The analyses are used to create a framework for a well-to-well correlation from which an
 110 explanation of aquifer thickness variations in the different doublets is proposed. This explanation is
 111 used to interpret regional aquifer architecture in different fault blocks.

112 **Data and Methods**

113 *Overview*

114 This study was based on a combination of seismic interpretation, Gamma-Ray (GR) log correlation,
115 and palynological analysis of cuttings. In the seismic interpretation, faults were identified in our study
116 area in the WNB, which were active during deposition of the Nieuwerkerk Formation. In combination
117 with a regional structural interpretation by Duin et al., (2006) the lateral extent of these faults was
118 identified. Secondly, by utilising palynological analyses of cuttings the chronostratigraphic position of
119 each aquifer sandstone interval was identified and MFS's were interpreted. This formed the
120 framework of improved geothermal GR well-log correlation. GR logs of eleven geothermal wells in
121 our study area were used to compare fluvial architecture in different fault blocks. All results were
122 finally combined in maps that predict the lateral extent of the sandstone-rich successions in the basin.
123 An overview of the data that was used in our study is presented in Figure 4.

124



125

126 *Figure 4: Location of the geothermal wells for the GR well-log correlation, cuttings analysis, the outline of the seismic cross-*
127 *section and the regional structural interpretation by Duin et al. (2006).*

128

129

130

131 *Structural setting of the Nieuwerkerk Formation*

132 On a seismic section perpendicular to the major fault trend, two seismic horizons were interpreted: the
133 top and base of the Nieuwerkerk Formation. The basin wide section was derived by merging ten 3D
134 seismic sections (Figure 4; Vondrak, 2016). Using horizon flattening of the top of the Formation, fault
135 blocks were identified that experienced different tectonic movement affecting fluvial architecture of
136 the Nieuwerkerk Formation. This is derived from thickness differences of the Formation between the
137 major faults. Using structural interpretation by Duin et al. (2006), the regional outlines of the fault
138 blocks that experienced different tectonic movement during deposition of the Nieuwerkerk Formation
139 were mapped. This result was used as the basis for regional well-log correlations and generation of
140 maps that describe the distribution of sandstone-rich successions.

141 *Palynological analysis*

142 A total of 42 cuttings samples from well PNA-GT-02, 40 samples from HON-GT-01 and 28 samples
143 from HON-GT-02 was analysed. Two additional samples from well VDB-GT-04 (at depth 1890 m
144 and 1910 m) complemented the palynological analysis of Munsterman (2012). The samples were
145 processed at the TNO laboratory using the standard sample processing procedures (e.g., Janssen and
146 Dammers, 2008), which involved HCl and HF treatment, and sieving over an 18 µm mesh sieve. The
147 well selection was based on the well location in different graben blocks and the total thickness of the
148 Nieuwerkerk Formation that these wells encountered. Larger total thickness could potentially reveal
149 more information from the fluvial interval. The cuttings descriptions and the GR logs in the ‘End-of-
150 well-reports’ (NLOG, 2017), in combination with results from Munsterman (2010) provided an basis
151 for the selection of sample depths. The location of the wells in different fault blocks allowed relating
152 differences in fluvial architecture to the syn-tectonic origin of the interval. The palynological analysis
153 consisted of age dating and identification of the *Elegans* MFS and the *Paratollia* MFS (e.g., Jeremiah
154 et al., 2010), which formed the framework of our regional correlation scheme.

155

156

157

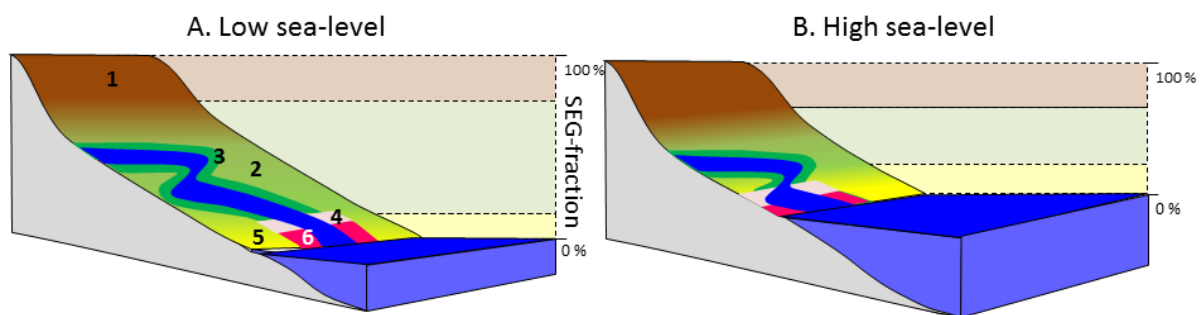
158 *Age dating*

159 The age interpretation was based on the Last Occurrence Datum (LOD) of palynomorphs, in particular
160 dinoflagellate cysts (dinocysts), and pollen and spores (sporomorphs). Key-references concerning the
161 palynostratigraphy of the Early Cretaceous from the North Sea region were: Abbink (1998), Costa and
162 Davey (1992), Davey (1979; 1982), Duxbury et al. (1999), Duxbury (2001), Heilmann-Clausen
163 (1987), Herngreen et al. (2000), Partington et al. (1993) and Riding and Thomas (1992). The
164 international geological time scale of Gradstein et al. (2012) was followed.

165

166 *Sporomorph Eco-Grouping (SEG) method*

167 The SEG method (Abbink, 1998; Abbink, 2001; Abbink et al., 2004A and 2004B) was used to identify
168 the Paratollia MFS in the fluvial aquifer interval of HON-GT-01, HON-GT-02, and PNA-GT-02. With
169 this method, sporomorph types were related to vegetation eco-groups. Abbink et al. (2004) classified
170 Jurassic to Lower Cretaceous sporomorphs into six eco-groups. (1) Upland vegetation grows on higher
171 terrain well above ground water level, which is never submerged by water. (2) Lowland vegetation is
172 found on plains with or without fresh water swamps. It is not influenced by salt water. When
173 periodically submerged it is referred to as 'Wet-Lowland' otherwise 'Dry-Lowland'. (3) River
174 vegetation is found on riverbanks and could be periodically submerged. (4) Pioneering vegetation
175 occupies recently developed eco-space that has been previously submerged by seawater. (5) Coastal
176 vegetation is found along the coast. (6) Tidally influenced vegetation is daily influenced by tidal
177 changes and regularly submerged in a salt-water regime. Quantitative analysis of sporomorphs
178 indicated percentages of eco-groups that were represented in the cuttings samples. In the SEG method
179 it is assumed that the lower coastal plain area is reduced during a transgression (Figure 5-A to B).
180 Therefore the relative share of Lowland eco-group vegetation is minimal on the moment of maximum
181 transgression, when a MFS is formed. Based on this assumption, trends in relative representation of
182 eco-groups were related to sea-level fluctuation. MFS's were assigned to samples where the relative
183 share of 'Upland' sporomorphs peaked with respect to the 'Lowland' eco-group while the marine
184 influenced eco-groups were poorly represented or absent. Cuttings samples with 10 m intervals were
185 analysed in the 2560 to 2810 m (MD) interval in HON-GT-01, 2590 to 2860 m (MD) in HON-GT-02
186 and 2440-2850 m (MD) in PNA-GT-02. These intervals were selected based on their fluvial origin
187 which was derived from the cuttings description in the 'End-of-well-reports' (NLOG, 2017).
188



189

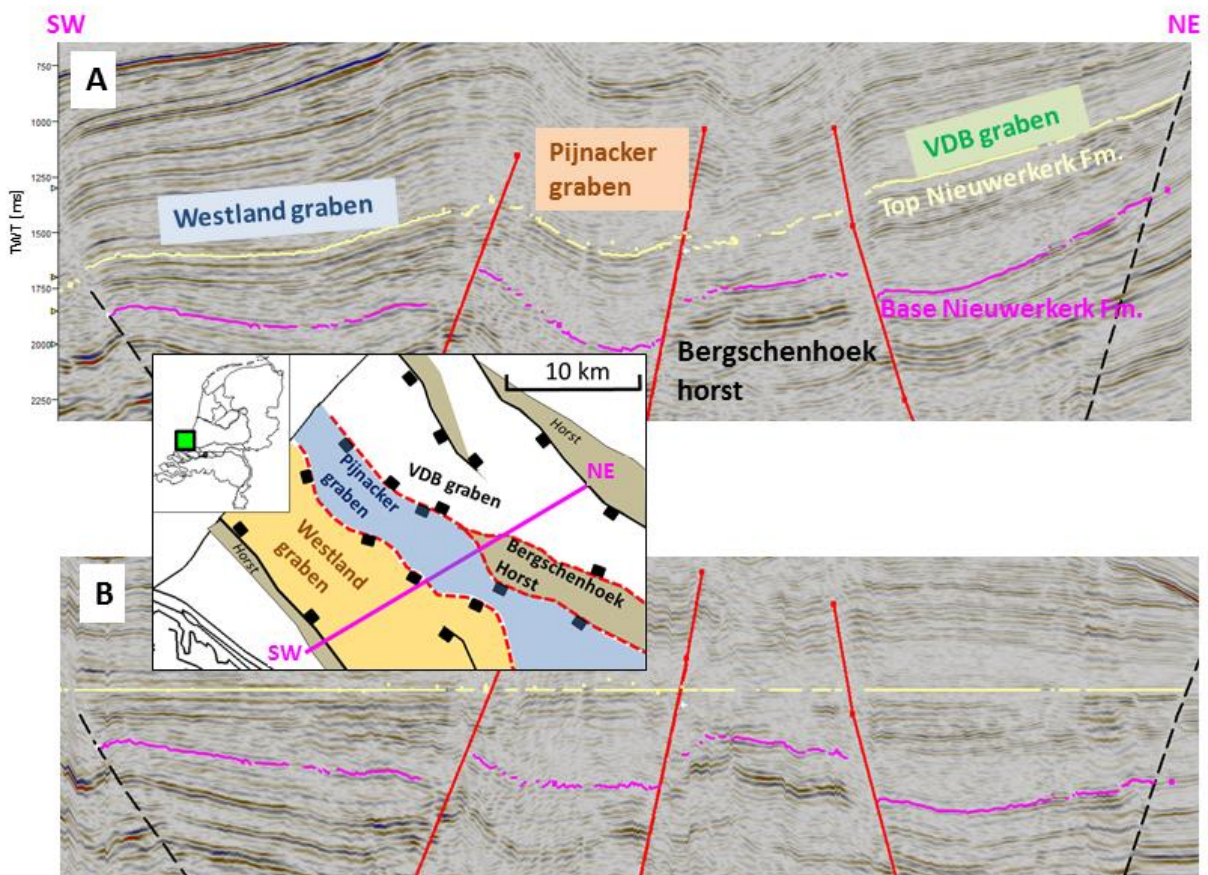
190 *Figure 5: Schematic representation of the impact of (A) low sea level and (B) high sea level on the relative occurrence of eco-*
191 *groups: 1=Upland, 2=Lowland, 3=River, 4=Pioneer, 5=Coastal, 6=Tidally influenced. Note the lower relative occurrence of the*
192 *'Lowland' eco group with high sea level in (B). Modified from Abbink et al. (2004a,b).*

193

194 **Results**

195 *Seismic interpretation*

196 On the seismic cross-section three half-grabens and one horst block were recognised (Figure 6-A). The
197 fault blocks were referred to as ‘Westland graben’, ‘Pijnacker graben’, ‘VDB graben’ and
198 ‘Bergschenhoek horst’. The interpretation of the top and base of the Nieuwerkerk Formation indicated
199 a lateral thickness variation of the Nieuwerkerk Formation in these grabens and horst, created by syn-
200 depositional fault movement. Horizon flattening of the Top Nieuwerkerk Formation horizon was
201 applied to highlight fault blocks where sedimentation might be affected by this tectonic movement
202 (Figure 6-B). The associated faults that were active during deposition of the formation are highlighted
203 in red. The regional extent of these faults was derived from the structural interpretation by Duin et al.
204 (2006). The three grabens are highlighted on the map in Figure 6. These results were used for the
205 comparison of fluvial reservoir architecture in these three fault blocks.
206



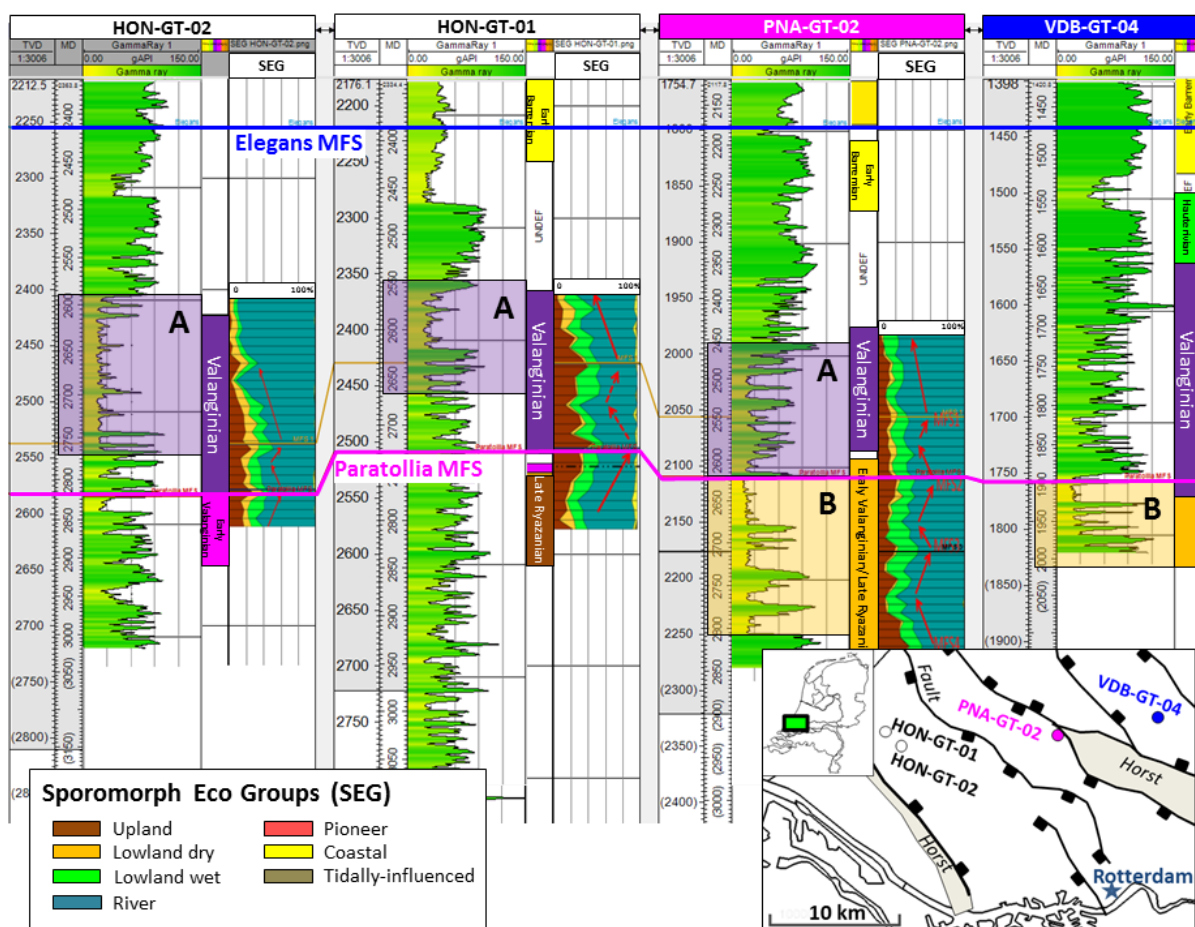
207
208 *Figure 6: (A) Seismic section with interpretation of faults as well as top (yellow) and base (pink) of the Nieuwerkerk*
209 *Formation horizons. (B) Horizon flattening on top Nieuwerkerk Formation. The outline of the seismic section and the outline*
210 *of the interpreted faults are indicated on the map.*

211

212 *Palynological analysis*

213 Palynological age dating formed the basis of the GR well-log correlation scheme. An overview of the
 214 results is presented in Figure 7 and Table 1. A detailed description of the analysis of all samples is
 215 presented in Appendix 1. Two MFS's were identified in HON-GT-01 and HON-GT-02 and four
 216 MFS's in PNA-GT-02. The MFS that is close to the Early Valanginian to Late Ryazanian boundary is
 217 associated with the Paratollia MFS in all wells. In well PNA-GT-02, this was based on the LOD of
 218 *Stiphrosphaeridium dictyophorum* (Sdi) at 2600 m and the LOD of *Canningia compta* (Cco) at depth
 219 2620 m (Appendix 1). In HON-GT-01, the Paratollia MFS was interpreted at depth 2730 m based on
 220 the LODs of *Canningia compta* (and a morphologically closely related *Escharisphaeridia* spp. at 2730
 221 m) and *Perisseiasphaeridium insolitum* at depth 2740 m MD (Costa and Davey, 1992; Strauss et al.,
 222 1993). In well HON-GT-02, this is based on the LOD of a single dinoflagellate cyst
 223 *Stiphrosphaeridium dictyophorum*.

224



225

226 *Figure 7: Combination GR logs, Palynological age dating of intervals and results of the SEG analysis. Age interpretation in*
 227 *VDB-GT-04 is based on Munsterman (2012). (A) Sandstone-rich zone of Valanginian age, (B) sandstone-rich zones of Early*
 228 *Valanginian/Late Ryazanian age.*

229

230 The palynofacies and their relative occurrence in both HON-GT wells and PNA-GT-02 indicate that
 231 the Valanginian to Late Ryazanian interval was formed in a relatively humid, fluvial lowland
 232 environment, not directly positioned close to the coast. This last observation is derived from the
 233 absence or rare recognition of marine indicators. Both the sandstone content and the relative
 234 occurrence of sporomorphs associated to the ‘Lowland-dry’ eco-group is higher in HON-GT-02
 235 compared to HON-GT-01, despite the relatively small distance of approximately 1.5 km between the
 236 wells in this doublet (Figure 7).

237
 238
 239
 240

Table 1: Overview of interval age dating.

Depth (m) MD	PNA-GT-02
2120-2175	Late Barremian
2195-2215	late Early Barremian, elegans Ammonite Zone or older
2235-2275	earliest Barremian variabilis Ammonite Zone or older
2440-2590	Valanginian
2600-2850	Late Ryazanian- Early Valanginian
	HON-GT-01
2320	Late Barremian
2340-2360	early Late Barremian
2380-2420	late Early Barremian, elegans Ammonite Zone or older
2560-2730	Valanginian
2740	Early/earliest Valanginian
2750-2810	Late Ryazanian, post-kochi Ammonite Zone
	HON-GT-02
2610-2820	Valanginian
2830-2860	Early Valanginian
	VDB-GT-04
1320-1530	Barremian (Munsterman, 2012)
1530-1625	Barremian - Hauterivian (Munsterman, 2012)
1625-1890	Valanginian (Munsterman, 2012)
1890-1910	Late Ryazanian- Early Valanginian

241
 242
 243
 244

245 In VDB-GT-04, the recognition of the *Paratollia* Ammonite Zone was based on the presence of
 246 *Perisseiasphaeridium insolitum*, *Stiphrosphaeridium dictyophorum*, *Canningia compta*,
 247 *Hystrichosphaeridium scoriaceum* and *Oligosphaeridium diluculum* in the samples at 1890 m and
 248 1910 m MD (Costa and Davey, 1992). A marine origin of the sample at 1890 m MD was recognised
 249 and therefore it may most likely be associated with the Paratollia MFS. Note that this is not based on
 250 SEG analysis in this well.

251
 252
 253
 254
 255
 256
 257
 258

The results indicate that the aquifers in the four wells are not part of a single sandstone-rich
 succession. At least two sandstone-rich zones are encountered of Valanginian and Ryazanian age with
 limited lateral extent (Figure 7). The Valanginian sandstone-rich zone A in HON-GT-01 relates to the
 upper section of the sandstone-rich zone in PNA-GT-02 with the same age. In contrast, the
 Valanginian succession in VDB-GT-04 is claystone-dominated. In this well, the aquifer is formed by a
 Ryazanian sandstone rich-zone B that relates to the Ryazanian sandstone-rich zone in PNA-GT-02. In
 HON-GT-01 the Ryazanian succession is claystone-dominated. Stacking of both sandstone-rich zones

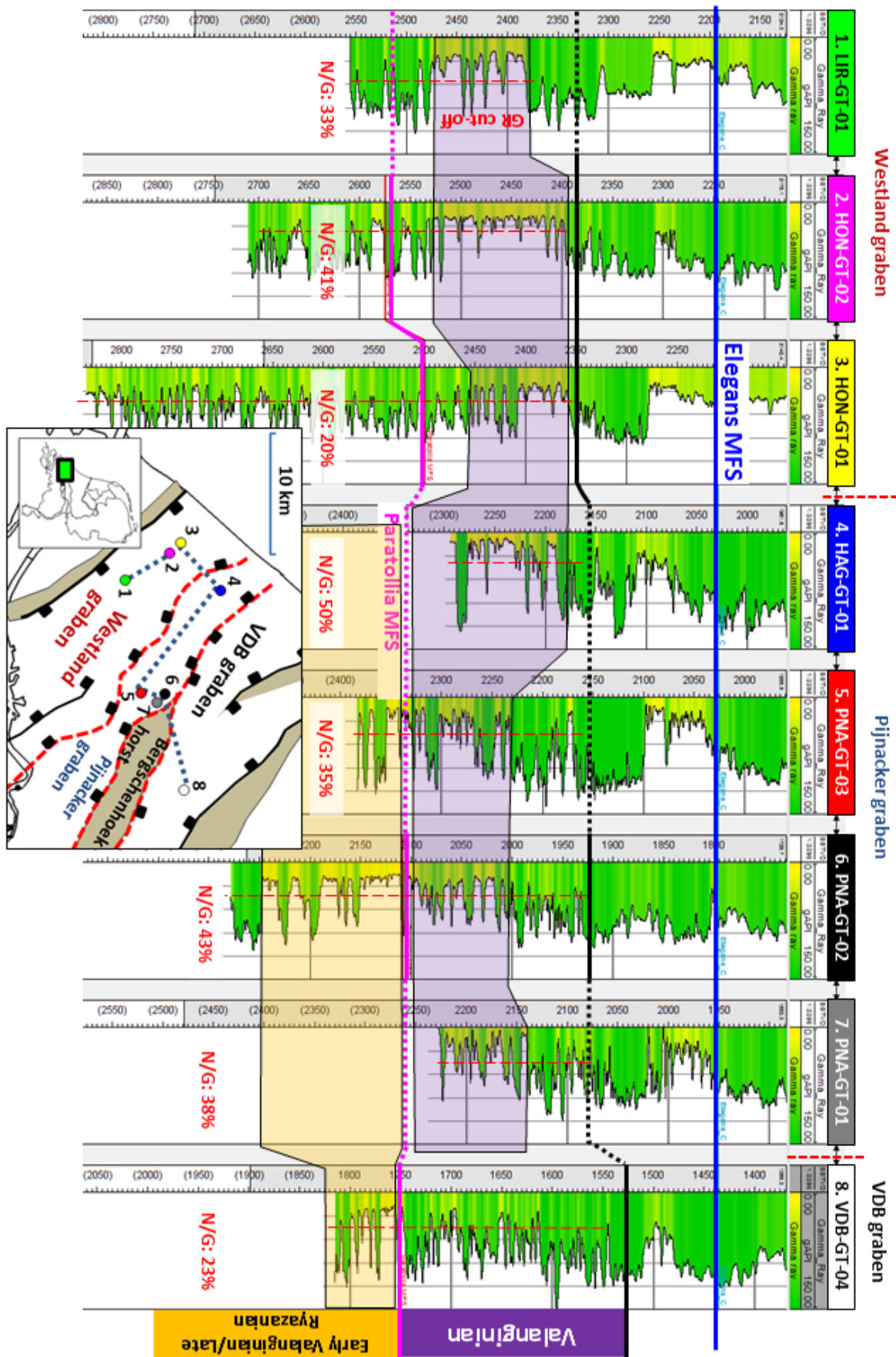
259 A and B accounts for the increased aquifer thickness in well PNA-GT-02. In contrast, lower aquifer
260 thickness could be explained by the presence of a single sandstone-rich zone in HON-GT-01 and
261 VDB-GT-04.

262

263 *Regional well-log correlation*

264 In the four wells with palynological analysis, the *Paratollia* MFS was recognised at approximately
265 300 m true vertical depth below the Elegans MFS (Figure 8). In the wells without palynological
266 cuttings analysis or in wells that did not reach sufficient depth, the top and base of the Valanginian
267 succession were interpreted by extrapolation GR log patterns assuming constant thickness of the
268 Valanginian interval. The resulting correlation scheme indicates that the Valanginian interval is
269 sandstone-rich in both the Westland and Pijnacker grabens. In contrast, this interval has low sandstone
270 content in the VDB fault block (Figure 8). The Early Valanginian/Ryazanian interval has a low
271 sandstone content in the Westland fault block, but high sandstone content in the Pijnacker and VDB
272 fault blocks. Our correlation scheme suggests that the prevailing position of the meander belts in
273 which sand was deposited shifted from the east to the west side of the basin during the Ryazanian and
274 Valanginian. In the Pijnacker fault block, both the Valanginian and the Early Valanginian/Ryazanian
275 intervals have a high sandstone content. This accounts for the largest interval with high sandstone
276 content in all geothermal wells in the basin of approximately 250 m thickness in the PNA-GT-02 well.
277 The other wells in this fault block have a limited total depth. Therefore they did not intersect the total
278 Early Valanginian/Ryazanian interval. Similarly, the limited total depth of the VDB-GT-04 well only
279 shows 70 m of the Early Valanginian/Ryazanian interval of which approximately 50 m is sandstone-
280 rich. In the Westland fault block, the Valanginian aquifer thickness ranges from 50 to 150 m. In the
281 HON-GT-01 well, the lower half of the Valanginian interval is claystone-rich, unlike the other wells.
282 The net-sandstone content (N/G) of the combined Valanginian and Early Valanginian intervals is
283 calculated for each well. A specific GR log cut-off value is used in each well to take the differences in
284 GR calibration into account. The N/G values range from 20% in the HON-GT-01 well where thick,
285 non-aquifer intervals are included in the calculation, to 50% in the HAG-GT-01 well where the N/G
286 calculation is based on the sandstone-dominated Valanginian interval. The arithmetic average N/G in all
287 wells of the combined Valanginian and Early Valanginian/Late Ryazanian intervals is 35%.

288



289
290
291

Figure 8: Well-log correlation of geothermal wells in three different fault blocks in the WNB. Solid lines indicate MFS interpretation based on cuttings analysis, dotted line is the projected MFS based on TVD, in wells without cuttings analysis.

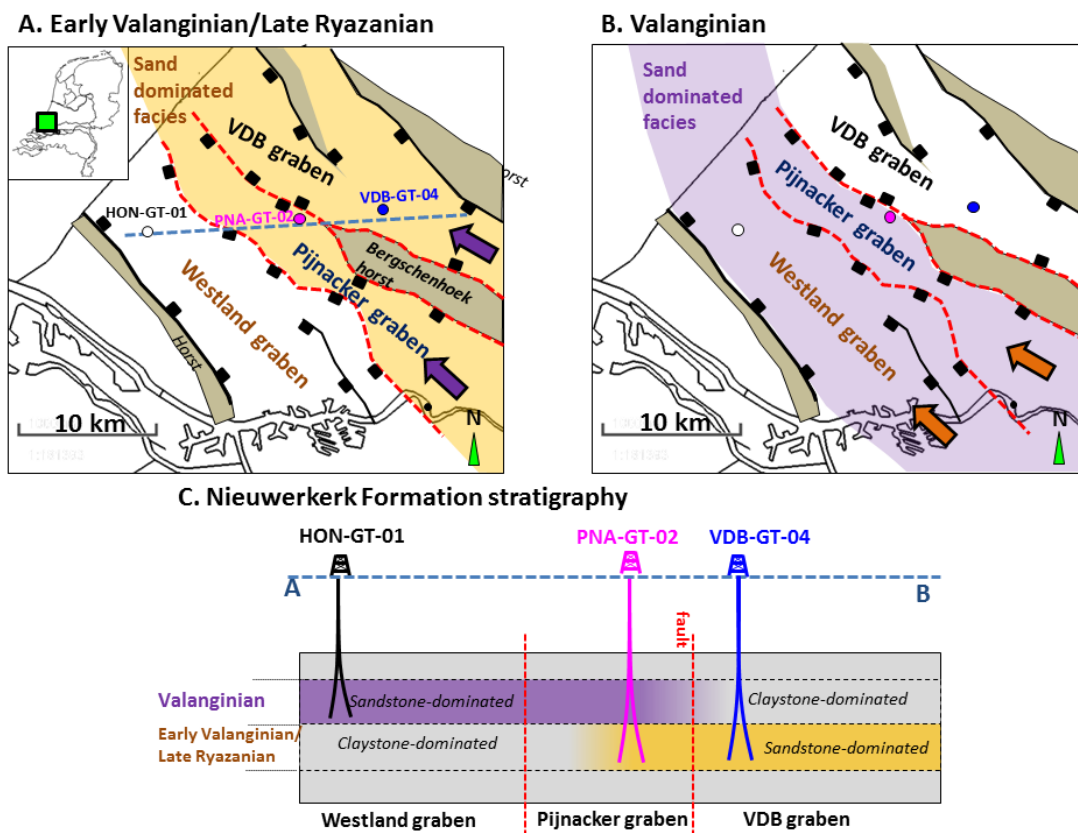
292 **Discussion**

293 *Ryazanian/Early Valanginian shift of sandstone-dominated facies*

294 The seismic facies interpretation of a regional westward shift of sandstone-dominated facies during the
 295 Valanginian (Den Hartog Jager, 1996) is corroborated by our palynology-based correlation (Figure 9).
 296 Because of the unidirectional nature of the shift in sandstone-dominated facies in our study, we
 297 propose a tectonic origin of the shift. In absence of such tectonic control, successive meander-belt
 298 avulsions and inherent compensational stacking would be the ruling processes, and a random spatial
 299 distribution of the fluvial sandstones the characteristic sedimentary architecture (e.g., Stouthamer and
 300 Berendsen, 2007; Hajek et al., 2010; Donselaar et al., 2013; Flood and Hampson, 2016; Van
 301 Tooreenburg et al., 2016). Based on this hypothesis, maps are generated that predict the lateral extent
 302 of the Ryazanian/Early Valanginian sandstone-rich zone (Figure 9-A) and the Valanginian sandstone-
 303 rich zone (Figure 9-B).

304 If tectonic movement had a strong impact on sedimentation, this might invalidate our
 305 assumption that the Valanginian interval has a constant thickness in our study area. In that case, it
 306 could be expected that the thickness of the Valanginian interval would increase in wells that are closer
 307 towards the hanging wall of grabens. However, we expect that this would not have a significant impact
 308 on the trend in Figure 8 for two reasons. Firstly, the geothermal wells in the ‘Pijnacker Graben’ and
 309 ‘Westland Graben’, are drilled more or less parallel to the major fault trend and therefore the thickness
 310 correction would affect them equally. Secondly, in the wells with our palynological analysis an
 311 approximately constant thickness was observed, despite the fact that the four geothermal wells are
 312 located in different fault blocks. Additional palynological analysis in other WNB doublets, could
 313 verify if the assumption is valid.

314



315
 316 *Figure 9: Series of maps indicating the location of sand-dominated sedimentation during the (A) Ryazanian / Early*
 317 *Valanginian and (B) Valanginian. Arrows indicate fluvial palaeoflow direction. (C) Cartoon illustrating facies distribution in*
 318 *the fluvial interval of the Nieuwerkerk Formation on a cross-section perpendicular to the fault trend.*

319 *Regional aquifer architecture*

320 In the present study, the correlation of the sandstone intervals in the Nieuwerkerk Formation are based
321 on their chronostratigraphic position and the occurrence of two MFS's, whereas previous studies used
322 a lithostratigraphic correlations. Van Adrichem Boogeaart and Kouwe (1993) identified the youngest
323 fluvial sandstone-rich interval in the Formation as the Delft Sandstone Member. Their regional aquifer
324 architecture model (Figure 2-A) is used in current geothermal exploitation in the basin but does not
325 adequately explain aquifer thickness variations like shown in Figure 1. DeVault and Jeremiah (2002)
326 described the regional aquifer architecture as a more random distribution of amalgamated sand
327 complexes with limited lateral continuity that occur throughout the Nieuwerkerk Formation. These
328 previous descriptions of the aquifer architecture were based on hydrocarbon wells on structural highs
329 in the basin. Previously aquifer thickness prediction in the grabens was uncertain without well control,
330 especially because these fault blocks might have experienced different tectonic movement. New well
331 data from the graben fault blocks and the palynological analysis of our study suggest the aquifer
332 architecture as sketched in Figure 9.

333 Because the number of geothermal wells in the grabens is still limited, the continuity of
334 sandstone complexes is still uncertain. In the entire fluvial Valanginian to Late Ryazanian interval,
335 N/G ranges from 20% to 50% with an arithmetic average of 35% (Figure 8). These percentages are
336 an initial estimate of N/G, as no sensitivity study of GR cut-off value is included. Nevertheless this
337 indicates that significant volumes of claystone are preserved. The Nieuwerkerk Formation is deposited
338 by a relatively small meandering fluvial system with a paleoflow depth of approximately 4 m (e.g.,
339 DeVault and Jeremiah, 2002). The associated paleo channel width and channelbelt width are therefore
340 estimated to be approximately 40 m and 1 to 2 km, respectively (e.g., Gibling, 2006, Bridge, 2006).
341 The maximum width of individual sandstone bodies is smaller than the channelbelt widths (e.g.,
342 Donselaar and Overeem, 2008, Donselaar et al., 2015). Through amalgamation sandstonebody width
343 might extend further. However, claystone bodies are likely to form flow baffles or barriers
344 perpendicular to the paleoflow direction. This should be taken into account in doublet design and
345 doublet placement as it will have an impact on possible interference between adjacent doublets and
346 flowpath formation between injection- and production wells of individual doublets (e.g., Willems et
347 al., 2017).

348 Our results have an impact on expected aquifer thickness in different fault blocks. Larger
349 aquifer thickness could be expected in the Pijnacker fault block where sandstone-dominated zones in
350 both succession overlap. Furthermore, our results affect expected aquifer depth and therefore drilling
351 costs in different fault blocks. As is illustrated in Figure 9-C, the aquifer is found at larger depth in the
352 VDB fault block compared to the other two fault blocks. In addition, our results can be used for
353 aquifer property extrapolation for new geothermal doublets. For example, the expected injectivity and
354 productivity of future doublets should be based more on values, which are measured in geothermal
355 doublets in the same fault block. It is also possible that stratigraphically different sandstone
356 successions have different properties. In current WNB doublets, productivity and injectivity vary
357 considerably (van Wees et al., 2012). However, the variation could also be due to other factors such as
358 scaling or skin formation. Van Wees et al. (2012) pointed out that unfortunately it is not possible to
359 identify a single cause of this variability because of limited available data.

360
361 *Palynological analyses and SEG method*

362 Comparison of our results with those of Munsterman (2012) shows that the Valanginian interval in
363 VDB-GT-04 has a relatively more lower coastal plain character with respect to the HON-GT doublet
364 and the PNA-GT-02 well. This could be due to a topographical difference between the fault blocks
365 during the Valanginian. The SEG analysis indicated that in the HON-GT-02 well, a relatively higher
366 fraction of 'Lowland-dry' type sporomorphs were recognised which could point at a more inland

367 location of the well compared to HON-GT-01 that is drilled more towards the paleo-coastline in the
368 north (e.g., Den Hartog Jager, 1996). The Valanginian interval of HON-GT-01 also has a higher
369 claystone content that could also be explained by a more near coastal location of this well. In addition,
370 the change in sandstone content could be explained by fault movement that directed the location of
371 sand-rich meander_belt deposits towards well HON-GT-02 while HON-GT-01 was located in the
372 floodplain region. Due to the limited number of wells in our study, it is currently unclear how these
373 observations are related to the fluvial architecture, sandstone distribution and the location of the paleo-
374 coastline.

375 The palynological age dating gives an indication of the age of interval and is not able to
376 identify exact age boundaries or the exact location of the Paratollia MFS. The resolution of the age
377 dating is limited by the sample spacing of 10 m and the risk of caving from higher sections.
378 Uncertainty in age interpretation applies most to the Valanginian - Late Ryazanian boundary in our
379 study area. Often, our interpretation of this boundary was based on the recognition of a limited number
380 of palynological indicators. In contrast, identification of the marine Elegans MFS has a lower degree
381 of uncertainty because it was based on a combination of GR log interpretation and palynological
382 analysis. This is because GR log signals in marine intervals are more often related to sea-level changes
383 compared to GR log signals in fluvial intervals, like the Valanginian to Late Ryazanian interval in our
384 study area. In addition marine dinoflagellate cysts provide a higher resolution dating than (long
385 ranging) terrestrial spores and pollen.

386 Our results underline the importance of palynological analysis for fluvial well-log correlation.
387 These analyses enabled the identification of markers within fluvial claystone-dominated as well as
388 sandstone-dominated successions, which would not have been possible based on GR log interpretation
389 alone.

390
391

392 **Conclusions**

393 Based on the results of this study we can conclude that:

- 394 • Current WNB geothermal doublets encounter sandstone-rich zones in at least two stratigraphic
395 intervals of Valanginian age and of Early Valanginian/Ryazanian age.
- 396 • Sandstone-rich zones in both intervals can overlap, which accounts for the large aquifer
397 thickness in the PNA-GT-02 well.
- 398 • Valanginian tectonic movement induced a shift of the deposition of sandstone-dominated
399 facies from the east to the west of the basin.
- 400 • This shift has an impact on expected aquifer thickness and aquifer depth in different fault
401 blocks in the basin.

402
403

404 **Acknowledgements**

405 This study was carried out by Delft University of Technology in collaboration with Panterra
406 Geoconsultants and TNO, in the context of the Research Agenda Geothermal Energy of the ministry
407 of Economic Affairs and LTO Glaskracht Nederland in the innovation program: 'Kas als
408 Energiebron'. We kindly thank the consortium of share- and stakeholders of the Delft Geothermal
409 Project (DAP) for their support. We thank the associate editor Geert-Jan Vis and the reviewers Daan
410 den Hartog Jager and Henk Kombrink for their constructive and helpful revisions of the original
411 manuscript.

412
413
414

415 **References**

- 416 Abbink, O.A., 1998. Palynological investigations in the Jurassic of the North Sea region. PhD thesis, Utrecht University.
417
- 418 Abbink, O.A., Targarona J., Brinkhuis, h., Visscher, H., 2001. Late Jurassic to earliest Cretaceous palaeoclimatic evolution
419 of the southern North Sea. *Global and Planetary Change* 30, pp. 231–256.
420
- 421 Abbink, O.A., Van Konijnenburg-Van Cittert, J.H.A., Van der Zwan, C.J., Visscher, H., 2004A. A sporomorph ecogroup
422 model for the NW European Jurassic-Lower Cretaceous. *Netherlands Journal of Geosciences*, 83(2), 81-92.
423
- 424 Abbink, O.A., Van Konijnenburg-Van Cittert, C.J., Visscher, H., 2004B. A sporomorph ecogroup model for the NW
425 European Jurassic-Lower Cretaceous: concepts and framework. *Netherlands Journal of Geosciences*, 83(1), 17-38.
426
- 427 Bridge, J.S., 2006. Fluvial Facies Models: Recent Developments. In: Posamentier, H.W., Walker, R.G. (eds.), *Facies Models*
428 *Revisited*. SEPM Special Publication, 84, pp. 85-170.
429
- 430 Costa, L.I., Davey, R.J., 1992. Dinoflagellate cysts of the Cretaceous System. In: Powell, A.J. (Ed.), *A Stratigraphic Index of*
431 *Dinoflagellate Cysts*, pp. 99-154.
432
- 433 Davey, R.J., 1979. The stratigraphic distribution of dinocysts in the Portlandian (latest Jurassic) to Barremian (Early
434 Cretaceous) of northwest Europe. *AASP, Contribution Series 5B*, pp. 48-81.
435
- 436 Davey, R.J., 1982. Dinocyst stratigraphy of the latest Jurassic to Early Cretaceous of the Haldager No. 1 borehole, Denmark.
437 *Geological Survey Denmark Series B*, 6, p. 58.
438
- 439 Den Hartog Jager, D. G., 1996. Fluvio-marine sequences in the Lower Cretaceous of the West Netherlands Basin: correlation
440 and seismic expression. In: H. E. Rondeel, D. A. J. Batjes, and W. H. Nieuwenhuijs, (eds.), *Geology of gas and oil under the*
441 *Netherlands*, Dordrecht, Kluwer Academic Publishers, 229–241.
442
- 443 Donselaar, M.E., Overeem, I., 2008. Connectivity of fluvial point-bar deposits: An example from the Miocene Huesca fluvial
444 fan, Ebro Basin, Spain. *AAPG Bulletin*, 92(9), 1109-1129.
445
- 446 Donselaar, M.E., Cuevas Gozalo, M.C., Moyano, S., 2013. Avulsion processes at the terminus of low-gradient semi-arid
447 fluvial systems: lessons from the Río Colorado, Altiplano endorheic basin, Bolivia. *Sedimentary Geology*, 283, 1-14.
448
- 449 Donselaar, M.E., Groenenberg, R.M., Gilding, D.T., 2015. Reservoir Geology and Geothermal Potential of the Delft
450 Sandstone Member in the West Netherlands Basin. In: *Proceedings World Geothermal Congress 2015*, Melbourne, Australia,
451 19-25 April 2015, 9 pp.
452
- 453 Duin, E.J.T., Doornenbal, J.C., Rijkers, R.H.B., Verbeek, J.W., Wong, Th.E., 2006. Subsurface structure of the Netherlands
454 – results of recent onshore and offshore mapping. *Netherlands Journal of Geosciences*, 85(4), 245-276.
455
- 456 Duxbury, S., Kadolsky, D., Johansen, S., 1999. Sequence stratigraphic subdivision of the Humber Group in the Outer Moray
457 Firth area (UKCS, North Sea). In: Jones, R.W., Simmons, M.D. (eds.), *Biostratigraphy in Production and Development*
458 *Geology*. Geological Society, London, Special Publication, 152, pp. 23-54.
459
- 460 Duxbury, S., 2001. A palynological zonation scheme for the Lower Cretaceous United Kingdom Sector, Central North Sea.
461 *N. Jahrbuch Geologisches Palaontologie Abhandlungen*, 219 (1), 95-137.
462
- 463 DeVault, B., Jeremiah, J., 2002. Tectonostratigraphy of the Nieuwerkerk Formation (Delfland Subgroup), West Netherlands
464 Basin, *AAPG Bulletin*, 86(10), 1679–1707.
465
- 466 Flood, Y.S., Hampson, G.J., 2015. Quantitative analysis of the dimensions and distribution of channelized fluvial sandbodies
467 within a large outcrop dataset: Upper Cretaceous Blackhawk Formation, Wasatch Plateau, central Utah, U.S.A. *Journal of*
468 *Sedimentary Research*, 85(4), 315-336.
469
- 470 Gibling, M.R., 2006. Width and thickness of fluvial channel bodies and valley fills in the geological record: A literature
471 compilation and classification. *Journal of Sedimentary Research*, 76, 731-770.
472

473 Gradstein, F., Ogg, J., Smith, A., Ogg, G.M., 2012. A geologic time scale. *Newsletters on Stratigraphy*, 45(2), 171–188.
474
475 Hajek, E.A., Heller, P.L., Sheets, B.A., 2010. Significance of channel-belt clustering in alluvial basins. *Geology*, 38(6), 535–
476 538.
477
478 Heilmann-Clausen, C., 1987. Lower Cretaceous dinoflagellate biostratigraphy in the Danish Central Trough. *Danmarks*
479 *Geologische Undersogelse Serie A (17)*, pp. 1-90.
480
481 Herngreen, G.F.W., Kerstholt, S.J., Munsterman, D.K., 2000. Callovian - Ryazanian ('Upper Jurassic') palynostratigraphy of
482 the Central North Sea Graben and Vlieland Basin, The Netherlands. *Mededelingen Nederlands Instituut voor Toegepaste*
483 *Geowetenschappen TNO*, 63.
484
485 Herngreen, G.F.W., Wong, T.E., 2007. Cretaceous. In: Wong, Th., Batjes, D.A.J., De Jager, J. (eds.), *Geology of the*
486 *Netherlands*. Royal Netherlands Academy of Arts and Sciences, Amsterdam, pp. 127–150.
487
488 Janssen, N.M.M., Dammers, G., 2008. Sample processing for pre-Quaternary palynology. TNO report 2008-UR1190/A.
489
490 Jeremiah, J.M., Duxbury, S., Rawson, P., 2010. Lower Cretaceous of the southern North Sea Basins: reservoir distribution
491 within a sequence stratigraphic framework. *Netherlands Journal of Geosciences*, 89(3/4), 203-237.
492
493 Krupnik, J., Ziaja, J., Barbacka, M., Feldman-Olszewska, A., Jarzynka, A., 2014. A palaeoenvironmental reconstruction
494 based on palynological analyses of Upper Triassic and Lower Jurassic sediments from the Holy Cross Mountains region.
495 *Acta Palaeobotanica*, 51(1), 35-65.
496
497 Munsterman, D.K., 2012. De resultaten van het palynologische onderzoek naar de ouderdom van de Onder Krijt successie in
498 boring Van den Bosch-04 (VDB-04), interval 925-2006 m. TNO report TNO-060-UT-2011-02200/B .
499
500 Mutterlose, J., Harding, I., 1987. Phytoplankton from the anoxic sediments of the Barremian (Lower Cretaceous) of North-
501 West Germany. *Abhandlungen der Geologischen Bundesanstalt*, 39, 177-215.
502
503 Partington, M.A.P., Copestake, P., Mitchener, B.C., Underhill, J.R., 1993. Biostratigraphic correlation of genetic stratigraphic
504 sequences in the Jurassic - lowermost Cretaceous (Hettangian - Ryazanian) of the North Sea and adjacent areas. In: Parker, J.,
505 (ed.), *Geological Society, London, Petroleum Geology Conference series*, 4, 371-386.
506
507 Pluymaekers, M.P.D., Kramers, L., Van Wees, J.-D., Kronimus, A., Nelskamp, S., Boxem, T., Bonté, D., 2012. Reservoir
508 characterisation of aquifers for direct heat production: Methodology and screening of the potential reservoirs for the
509 Netherlands. *Netherlands Journal of Geosciences* 91(4), 621-636.
510
511 Racero-Baena, A., Drake, S., 1996. Structural style and reservoir development in the West Netherlands oil province. In: H.
512 Rondeel, D. Batjes, Nieuwenhuijs, W., (eds.), *Geology of Gas and Oil under the Netherlands*. Kluwer Academic Publishers,
513 Dordrecht, pp. 211-229.
514
515 Riding, J.B., Thomas, J.E., 1992. Dinoflagellate cysts of the Jurassic System. In: Powell, A.J. (ed.), *A Stratigraphic Index of*
516 *Dinoflagellate Cysts*. Kluwer Academic Publishers, Dordrecht, pp. 7-98.
517
518 Shanley, K.W., McCabe, P.J., 1994. Perspectives on the sequence stratigraphy of continental strata. *AAPG Bulletin*, 78,
519 554–568.
520 Stouthamer, E., Berendsen, H.J.A., 2007. Avulsion, the relative roles of autogenic and allogenic processes. *Sedimentary*
521 *Geology*, 198(3), 309-325.
522
523 Strauss, C., Elstner, F., du Chene, R.J., Mutterlose, J., Reiser, H., Brandt, K.-H., 1993. New micropaleontological and
524 palynological evidence on the stratigraphic position of the "German Wealden" in NW Germany. *Zitteliana*, 20, 389-401.
525
526 NLOG, 2017. *Nl olie- en gasportaal*, www.nlog.nl.
527
528 Van Adrichem Boogaert, H.A., Kouwe, W.F.P., 1993. Stratigraphic nomenclature of the Netherlands, revision and update by
529 Rijks Geologische Dienst (RGD) and Netherlands Oil and Gas Exploration and Production Association (NOGEP):
530 *Mededelingen Rijks Geologische Dienst* 50, 1-180.
531

532 Van Tooreenburg, K.A., Donselaar, M.E., Noordijk, N.A., Weltje, G.J., 2016. On the origin of crevasse-splay amalgamation
533 in the Huesca fluvial fan (Ebro Basin, Spain): Implications for connectivity in low net-to-gross fluvial deposits. *Sedimentary*
534 *Geology*, 343, 156-164.
535
536 Van Wees, J.D.A.M., Degens, G., Zijp, M., De Boer, J., Obdam, A., Eyvazi, F.J., 2012. BIA Geothermal – TNO Umbrella
537 Report into the Causes and Solutions to Poor Well Performance in Dutch Geothermal Projects. TNO report, TNO 2012
538 R10719.
539
540 Vondrak, A., 2016. (Bio-) stratigraphic correlation of geothermal aquifers in the West Netherlands Basin. Panterra
541 Geoconsultants report, <https://www.kasalsenergiebron.nl/duurzame-energie/aardwarmte> (December, 2016).
542
543 Willems, C.J.L., Nick, H.M., Donselaar, M.E., Weltje, G.J., Bruhn, D.F., 2017. On the connectivity anisotropy in fluvial Hot
544 Sedimentary Aquifers and its influence on geothermal doublet performance. *Geothermics*, 65, 222-233.
545
546 Yoshida, S., 2000. Sequence and facies architecture of the upper Blackhawk Formation and the Lower Castlegate Sandstone
547 (Upper Cretaceous), Book Cliffs, Utah, USA. *Sedimentary Geology*, 136, 239-276.